Chemical Mechanism of Homoisocitrate Dehydrogenase from *Saccharomyces cerevisiae*[†]

Ying Lin,[‡] Jerome Volkman,[‡] Kenneth M. Nicholas,[‡] Takashi Yamamoto,[§] Tadashi Eguchi,[§] Susan L. Nimmo,[‡] Ann H. West,[‡] and Paul F. Cook*,[‡]

Department of Chemistry and Biochemistry, University of Oklahoma, 620 Parrington Oval, Norman, Oklahoma 73019, and Department of Chemistry and Materials Science, Tokyo Institute of Technology, O-okayama, Meguro-ku, Tokyo 152-8551, Japan

Received November 30, 2007; Revised Manuscript Received February 11, 2008

ABSTRACT: Homoisocitrate dehydrogenase (HIcDH, 3-carboxy-2-hydroxyadipate dehydrogenase) catalyzes the fourth reaction of the α-aminoadipate pathway for lysine biosynthesis, the conversion of homoisocitrate to α-ketoadipate using NAD as an oxidizing agent. A chemical mechanism for HIcDH is proposed on the basis of the pH dependence of kinetic parameters, dissociation constants for competitive inhibitors, and isotope effects. According to the pH−rate profiles, two enzyme groups act as acid–base catalysts in the reaction. A group with a pK_a of 6.5–7 acts as a general base accepting a proton as the β-hydroxy acid is oxidized to the β-keto acid, and this residue participates in all three of the chemical steps, acting to shuttle a proton between the C2 hydroxyl and itself. The second group acts as a general acid with a pK_a of 9.5 and likely catalyzes the tautomerization step by donating a proton to the enol to give the final product. The general acid is observed in only the V pH−rate profile with homoisocitrate as a substrate, but not with isocitrate as a substrate, because the oxidative decarboxylation portion of the isocitrate reaction is limiting overall. With isocitrate as the substrate, the observed primary deuterium and ^{13}C isotope effects indicate that hydride transfer and decarboxylation steps contribute to rate limitation, and that the decarboxylation step is the more rate-limiting of the two. The multiple-substrate deuterium/^{13}C isotope effects suggest a stepwise mechanism with hydride transfer preceding decarboxylation. With homoisocitrate as the substrate, no primary deuterium isotope effect was observed, and a small ^{13}C kinetic isotope effect (1.0057) indicates that the decarboxylation step contributes only slightly to rate limitation. Thus, the chemical steps do not contribute significantly to rate limitation with the native substrate. On the basis of data from solvent deuterium kinetic isotope effects, viscosity effects, and multiple-solvent deuterium/^{13}C kinetic isotope effects, the proton transfer step(s) is slow and likely reflects a conformational change prior to catalysis.

Homoisocitrate dehydrogenase (3-carboxy-2-hydroxyadipate dehydrogenase, EC 1.1.1.87) (HIcDH)[1] catalyzes the fourth reaction of the α-aminoadipate pathway (AAA) for lysine synthesis (*1*), the conversion of homoisocitrate (HIc) to α-ketoadipate (α-Ka) using NAD as an oxidant.

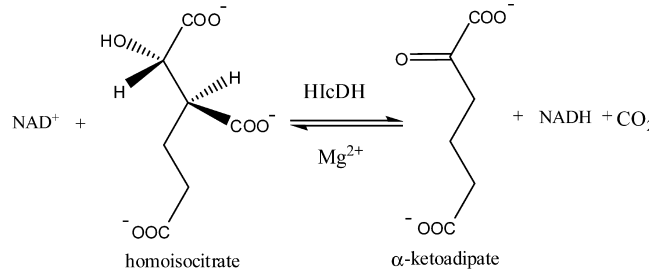

The kinetic mechanism of the HIcDH reaction has recently been determined from initial velocity studies in the absence and presence of product and dead-end inhibitors. HIcDH catalyzes a steady-state mechanism with random addition of MgHIc and NAD, but with a preferred ordered release of CO_2, α-Ka, and NADH (*2*).

HIcDH is a member of the family of pyridine nucleotide-linked β-hydroxy acid oxidative decarboxylases that includes the well-studied isocitrate dehydrogenase (IcDH), which catalyzes the oxidative decarboxylation of isocitrate, which

[†] This work was supported by Grant HR07-016 from the Oklahoma Center for the Advancement of Science and Technology (to P.F.C.), Grant GM 071417 from the National Institutes of Health (to P.F.C. and A.H.W.), and the Grayce B. Kerr Endowment to the University of Oklahoma (to support the research of P.F.C.).

* To whom correspondence should be addressed. E-mail: pcook@ou.edu. Telephone: (405) 325-4581. Fax: (405) 325-7182.

[‡] University of Oklahoma.

[§] Tokyo Institute of Technology.

[1] Abbreviations: HIcDH, homoisocitrate dehydrogenase; AAA, α-aminoadipate pathway; α-Ka, α-ketoadipate; NAD, nicotinamide adenine dinucleotide (the charge is omitted for convenience); NADH, reduced nicotinamide adenine dinucleotide; NADD, reduced nicotinamide adenine dinucleotide with deuterium in the 4(*R*) position; IcDH, isocitrate dehydrogenase; IPMDH, isopropylmalate dehydrogenase; TDH, tartrate dehydrogenase; 6-PGDH, 6-phosphogluconate dehydrogenase; GPDH, α-glycerophosphate dehydrogenase; HIc, 2(*R*),3(*S*)-homoisocitrate; Ic-2d, *threo*-D,L-[2-^{2}H]isocitrate; Ic, *threo*-D,L-isocitric acid; Hepes, *N*-(2-hydroxyethyl)piperazine-*N*′-2-ethanesulfonic acid; Ches, 2-(*N*-cyclohexylamino)ethanesulfonic acid; Bis-Tris, bis(2-hydroxyethyl)imino-tris(hydroxymethyl)methane; Tris, tris(hydroxymethyl)aminomethane; CMP, 3-carboxypropylidenemalate; MgHIc, chelate complex of magnesium and homoisocitrate; D_2O, deuterium oxide; DCl, deuterium chloride; NaOD, sodium deuterioxide; AcOEt, ethyl acetate; SKIE, solvent kinetic isotope effect.

10.1021/bi702361j CCC: $40.75
Published on Web 03/06/2008

Scheme 1: Proposed Chemical Mechanism for HIcDH

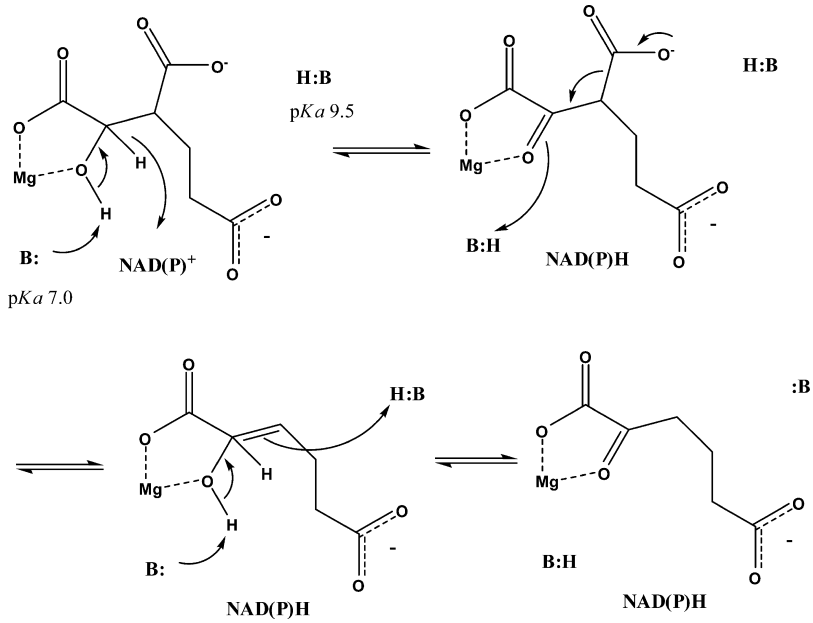

is structurally similar to HIc (*3*). On the basis of the known chemical mechanism of IcDH (*4*), a general mechanism can be proposed for HIcDH (Scheme 1). Once NAD and MgHIc are bound, the first chemical step is the oxidation of the β-hydroxy acid catalyzed by an enzymic general base and using NAD as the oxidant to produce α-keto-β-carboxyadipate. Decarboxylation of the β-keto intermediate then occurs using Mg^{2+} as a Lewis acid, with the general base now acting as a general acid to give the enol. Finally, general acid−general base-catalyed tautomerization of the enol gives the final ketone product. In the final step, the base that originally accepted the proton functions as a base while a second enzyme residue serves as an acid. Although the overall chemistry of the enzymes in this class is similar, the individual members of the class, including IPMDH (*5, 6*), malic enzyme (*7, 8*), TDH (*9*), and 6-PGDH (*10, 11*), catalyze their reaction differently. Malic enzyme utilizes a catalytic triad comprised of aspartate, lysine, and tyrosine to catalyze its reaction (*12*), while 6-PGDH, a metal ion-independent catalyst, uses lysine as a general base and glutamate as a general acid (*13, 14*). Other enzymes in the class have not been studied sufficiently thoroughly to know their acid–base mechanism in sufficient detail, even though structures and significant kinetic data are available.

In this paper, the pH dependence of kinetic parameters, dissociation constants for competitive inhibitors, and isotope effects are used to probe the chemical mechanism of HIcDH. On the basis of the data that were obtained, an overall mechanism is proposed and described in comparison to those of other members of the class of β-hydroxy acid oxidative decarboxylases.

MATERIALS AND METHODS

Chemicals. threo-D,L-Isocitrate, baker's yeast alcohol and aldehyde dehydrogenases, porcine heart isocitrate dehydrogenase, glutathione reductase, dihydroxyacetone phosphate (DHAP), and α-glycerophosphate dehydrogenase from rabbit muscle (GPDH) were obtained from Sigma. β-NADH, β-NAD, and LB broth were purchased from USB. Bis-Tris, Hepes, Ches, and Tris buffers were from Research Organics, Inc. Deuterium oxide (D_2O, 99 at. % D) and ethanol-d_6 (99 at. % D) were purchased from Cambridge Isotope Labotories, Inc. The nickel−nitrilotriacetic acid (Ni−NTA) agarose resin was from Qiagen. AG MP-1 and Bio-Gel P-2 resins were from Bio-Rad. The A-side NADD was synthesized according to the method of Viola et al. (*15*). α-Ketoadipate was prepared according to a published procedure (*2*).

Synthesis of 2(R),3(S)-Homoisocitric Acid. 2(*R*),3(*S*)-Homoisocitric acid was prepared by a known method (*16*). The diastereoselective allylation of dimethyl-D-malate was followed by the protection of the alcohol with acetyl chloride and a one-pot hydroboration−oxidation sequence. The triester thus obtained was saponified with KOH to yield the desired product. Preparative RP-HPLC was used for further purification in a 3% methanol/0.1% trifluoroacetic acid aqueous solution. The overall yield was 9%.

Synthesis of threo-D,L-Isocitric Acid-2d. threo-D,L-[2-^{2}H]Isocitric acid was prepared according to a known procedure (*17*) with slight modifications. Triethyl oxalosuccinate was prepared by the method of Friedman and Kosower (*18*) and reduced with $NaBD_4$. The product was purified by flash chromatography on silica gel (3:7 AcOEt/hexane mixture) to produce *threo*-D,L-[2-^{2}H]-3-ethoxycarbonyl-2-hydroxypentanedioic acid diethyl ester. Some residual *erythro* isomer was detected by ^{1}H NMR (∼20%).

threo-D,L-[2-^{2}H]-3-Ethoxycarbonyl-2-hydroxypentanedioic acid diethyl ester was hydrolyzed in 1 M NaOH by refluxing for 10 min. The reaction mixture was stirred at room temperature with Dowex 50WX8-100 resin and filtered; the filtrate was evaporated under vacuum to dryness. ^{1}H NMR (300 MHz, methanol-d_6) gave the following: δ 3.37 (dd, $J_1 = 5.4$ Hz, $J_2 = 9.3$ Hz, C3-H), 2.78 (dd, $J_1 = 9.3$ Hz, $J_2 = 17.1$ Hz, C4-H), 2.58 (dd, $J_1 = 4.8$ Hz, $J_2 = 16.8$ Hz, C4-H).

Enzyme Assays. The activity of HIcDH was measured by monitoring the increase or decrease in absorbance at 340 nm as NAD is reduced or NADH is oxidized using a Beckman DU 640 spectrophotometer. All assays were carried out at 25 °C, and the temperature was maintained with a

Neslab RTE-111 circulating water bath. A unit of enzyme activity is defined as the amount of enzyme catalyzing the production or utilization of 1 μmol of NADH/min at 25 °C. With HIc as a substrate, rate measurements were carried out in 0.5 mL of 50 mM Hepes (pH 7.5). Reactions were initiated by addition of 5 μL of an appropriately diluted enzyme solution (0.15 mg/mL) to a mixture that contained all other reaction components, and the initial linear portion of the time course was used to calculate the initial velocity. With isocitrate used as a substrate, reactions were initiated by adding 50 μL of an enzyme solution (protein concentration of 1.5 mg/mL), and all other conditions are as for assays with HIc.

pH Studies. To obtain an estimate of the K_m values of each of the substrates as a function of pH and to determine whether the kinetic mechanism changes with pH, initial velocity patterns were measured as a function of pH with the concentration of NAD varied at different fixed levels of MgHIc (or Ic). With HIc as a substrate, the pH dependence of *V* and *V*/*K* for all substrates was obtained from the initial velocity patterns described above. With Ic as the substrate, the pH dependence of *V* and *V*/*K* for all substrates was determined under conditions in which one substrate concentration was varied and the others were maintained at saturation ($\geq 10K_m$). Inhibition constants were obtained for inhibitors competitive with HIc at a fixed concentration of the other substrate ($10K_m$) and different fixed levels of inhibitor, including zero.

With HIc used as a substrate, the pH was maintained using the following buffers at a concentration of 100 mM: Bis-Tris, pH 5.0–6.8; Hepes, pH 6.8–8.2; Ches, pH 8.2–10.0 (with isocitrate, Tris buffer replaced Ches). Sufficient overlap resulted with the change in buffers for detection of buffer effects; none were observed. All reaction mixtures contained 0.2 M KCl. The ionic strength of the reaction mixtures over the pH range of our measurements is approximately constant at 0.3. The pH was recorded before and after initial velocity data were measured with observed changes limited to ≤ 0.1 pH unit. The enzyme is stable when incubated for at least 15 min over the pH range of 5.0–10.0. pH−rate profiles were evaluated graphically for quality of data by plotting log *V* or log(*V*/*K*) versus pH, while the inhibition profiles for Ic or 3-carboxypropylidenemalate (CPM) versus MgHIc (Figure 1) were evaluated by plotting log($1/K_i$) versus pH.

Primary Substrate Deuterium Kinetic Isotope Effects. With HIc as a substrate, isotope effects were measured in the direction of reductive carboxylation by direct comparison of initial velocities at pH 7.0 and 7.5, the pH-independent range of the *V* and *V*/*K* pH−rate profile, with A-side NADD used as the deuterated substrate. $^{D}V_2$ and $^{D}(V_2/K_{CO_2})$ were obtained by measuring the initial rate as a function of CO_2 concentration at saturating levels of NADH(D) ($10K_m$) and α-Ka ($20K_m$). Isotope effects were also measured via a comparison of initial rates at pH 6.23 and 9.5 as a function of NADH(D) concentration with α-Ka and CO_2 fixed at their respective K_m values.

With isocitrate-2d, isotope effects were measured at pH 8.0. $^{D}V_1$ and $^{D}(V_1/K_{Ic})$ were obtained by measuring the initial rate as a function of isocitrate-2-(h,d) concentration at saturating levels of NAD ($10K_m$), while $^{D}(V_1/K_{NAD})$ was obtained by varying the NAD concentration at saturating levels of isocitrate-2-(h,d).

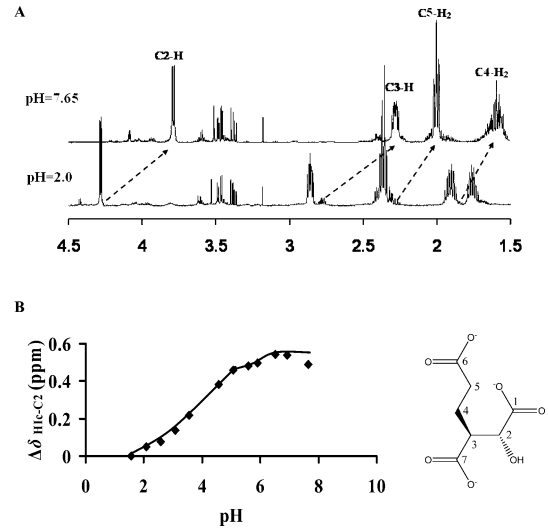

FIGURE 1: (A) ^{1}H NMR spectra of HIc obtained at pH 2.0 and 7.65. The chemical shifts of HIc were assigned by gCOSY. The dotted arrows show the shift of peaks corresponding to C(2)-H, C(3)-H, C(4)-H_2, and C(5)-H_2 from pH 2.0 to 7.65. (B) Titration of Hic monitoring the change in chemical shift of the C(2)-H proton. The curve exhibits the sum of two titrations, one from pH 1 to 6 and another from pH 6 to 7.5. The half-points for the two titrations estimated from the curve are approximately 4.2 and 5.8, respectively. The points are experimental. The numbering system used is that shown in the structure of Hic.

Effects of Solvent Deuterium and Viscosity. Initial velocities were measured in H_2O and D_2O. For rates measured in D_2O, substrates (HIc and Ic) and buffers were first dissolved in a small amount of D_2O and lyophilized overnight to remove exchangeable protons. The lyophilized powders were then dissolved in D_2O to give the desired concentrations, and the pD was adjusted using either DCl or NaOD. A value of 0.4 was added to the pH meter reading to calculate pD (*19*). Data were obtained by varying one substrate at a fixed concentration ($10K_m$) of the other. The isotope effects were obtained by direct comparison of initial rates in H_2O and D_2O at pH(D) 8.0 which is in the pH-independent range of the *V* and *V*/*K* pH−rate profiles. With HIc as the substrate, reactions were initiated by adding 5 μL of the enzyme solution (0.15 mg/mL) in H_2O so that the final percentage of D_2O was 99%. Similar experiments were carried out for the isocitrate reaction; however, 50 μL of the enzyme solution (2.5 mg/mL) in H_2O was added to initiate the reactions so that the final percentage of D_2O was 90%.

Initial velocities were determined in H_2O at a relative viscosity of 1.24 at pH 8.0 and 25 °C. Assays contained 9% glycerol (w/v) as the viscosogen, which generates the same relative viscosity as 100% D_2O at 25 °C (*20*). The amount of glycerol required to achieve a relative viscosity of 1.24 was determined by constructing a standard curve of the viscosity versus percent glycerol (*21*) and determining the required amount of glycerol from the linear standard curve.

For viscosity dependence studies with HIc as a substrate, the *V* and *V*/*K* for HIc and NAD were measured in the absence of glycerol and in the presence of 9, 18, or 27% glycerol as a viscosogenic agent.

^{13}C Kinetic Isotope Effects. The technique employed for the determination of ^{13}C isotope effects is that of O'Leary (*22*) in which the natural abundance of ^{13}C in the C4 position of HIc or Ic is used. Both high-conversion (100% reaction)

and low-conversion samples were collected. The ^{12}C:^{13}C isotope ratios in the CO_2 produced in the reactions were determined for both samples. From these ratios, the relative rates of reaction for ^{12}C versus ^{13}C, and thus the ^{13}C isotope effect, were calculated (*23*). Use of this natural abundance method minimizes the errors caused by atmospheric CO_2 contamination. With Ic as a substrate, reaction mixtures for the low-conversion reactions contained the following in 33 mL: 100 mM Hepes (pH 8.0), 20 mM isocitrate-2-(h,d), 5 mM $MgCl_2$, 200 mM KCl, and 10 mM NAD. Reaction mixtures for high-conversion reactions contained the following in 33 mL: 70 mM Hepes (pH 8.0), 2 mM isocitate-2-(h,d), 0.6 mM $MnSO_4$, 0.5 mM NADP, and 10 mM oxidized glutathione. The reaction mixtures were sparged with CO_2-free nitrogen overnight. Aliquots were withdrawn prior to the reaction to determine the initial concentration of isocitrate-2-(h,d) by an end point assay using IcDH. The low-conversion reactions were then initiated by the addition of 300 μL of the HIcDH solution (protein concentration of 12 mg/mL). The high-conversion reactions were initiated by the addition of 0.4 units of ICDH and 100 units of glutathione reductase.

With HIc as a substrate, reaction mixtures for the low-conversion reactions contained the following in 33 mL: 100 mM Hepes (pH 8.0), 20 mM HIc, 5 mM $MgCl_2$, 200 mM KCl, and 12 mM NAD. Reaction mixtures for high-conversion reactions contained the following in 33 mL: 100 mM Hepes (pH 8.0), 2 mM HIc, 5 mM $MgCl_2$, 200 mM KCl, and 10 mM NAD. The reaction mixtures were sparged with CO_2-free nitrogen overnight. Aliquots were withdrawn prior to reaction to determine the initial concentration of HIc by an end point assay using HIcDH. The low-conversion reactions were then initiated by the addition of 300 μL of the HIcDH solution (protein concentration of 0.15 mg/ml). The high-conversion reactions were initiated by the addition of 300 μL of the HIcDH solution (3.36 mg/mL). The ^{13}C isotope effects with HIc as a substrate were also measured in D_2O in the same manner.

Low-conversion reactions were quenched with 0.1 mL of concentrated sulfuric acid at the appropriate time. The extent of the reaction was determined by assessing the remaining Ic or HIc for aliquots of the reaction after quenching. The high-conversion samples were allowed to react overnight to ensure completion, which was confirmed by an end point assay prior to addition of 0.1 mL of concentrated sulfuric acid. Isolation of CO_2 was then carried out, and the isotopic composition of CO_2 was determined on an isotope ratio mass spectrometer (Finnigan Delta E). All ratios were corrected for ^{17}O according to the method of Craig (*24*).

Measurement of the HIc pK_a by ^{1}H NMR. The pK_a values of HIc were determined by measuring the ^{1}H NMR chemical shift of C(2)-H [or C(3)-H] of HIc as a function of pH at 21 °C. A solution in D_2O of 10 mM HIc was prepared. The solution was adjusted to different pD values (1.97–8.05) using either DCl or NaOD. A value of 0.4 was added to pH meter readings (*19*). All NMR experiments were performed on a Varian Mercury VNMRS 500 MHz spectrometer with a Varian triple-resonance indirect detection PFG probe. ^{1}H NMR one-dimensional (1D) spectra were collected using the PRESAT pulse sequence supplied by Varian, Inc. The spectra were collected with a sweep width of 7503.12 Hz and 128 transients. Assignments were made by two-dimensional (2D) gCOSY experiments. The gCOSY pulse sequence was provided by Varian, Inc., using one scan and 512 increments, with a sweep width of 8012.8 Hz.

Stereochemistry of Hydride Transfer to NAD. The A-side NADD was prepared according to the method of ref (*15*). The reaction mixture contained 7.6 mM ethanol-d_6, 6 mM NAD, 100 units of yeast alcohol dehydrogenase, and 100 units of yeast aldehyde dehydrogenase in 15 mL of 6 mM Taps, at pH 9.0 and 25 °C. The pH was adjusted to 9.0 with KOH throughout the reaction. The reaction proceeded overnight, and then 0.5 mL of $CHCl_3$ was added to the mixture to quench the reaction. The aqueous layer was adjusted to pH 10.0 with KOH and removed for ion-exchange chromatography. The NADD eluted in a large single peak with baseline separation from NAD when eluted isocratically from an AG MP-1 column with 0.2 M LiCl in 100 mM Ches buffer (pH 10.0). The ratio of absorbance at 260 and 340 nm obtained for the sample prepared in the manner described above is 2.3 ± 0.1, while that reported for A-side NADD is 2.15 ± 0.05 (*15*) . The purified NADD was concentrated by rotary evaporation to 20 mL, giving a final concentration of 4.33 mM.

To obtain NAD-4d, 32 units of GPDH was added to assay mixtures (16 mL) containing 2.5 mM A-side NADD, 7.5 mM DHAP, and 100 mM Hepes (pH 7.4). The reaction was allowed to proceed for 1–2 h and then quenched with 0.5 mL of $CHCl_3$. The aqueous layer was loaded onto an AG MP-1 column with 0.2 M LiCl in 100 mM Ches buffer (pH 8.05). The eluted NAD-4d peak was collected and concentrated by rotary evaporation to a volume of 20 mL. The concentrated solution was then desalted via a Bio-Gel P-2 column with 50 mM KH_2PO_4 buffer (pH 7.2). The purified NAD-4d was concentrated by rotary evaporation to 12 mL, giving a final concentration of 2.6 mM.

The synthesized NAD-4d was used to determine the stereochemistry of hydride transfer to NAD catalyzed by HIcDH. HIcDH (500 μL, 2 mg/mL) was added to a reaction mixture (12 mL) consisting of 3 mM MgHIc, 2 mM NAD-4d, 200 mM KCl, and 100 mM Hepes (pH 7.5). After incubation at room temperature for 7 h, the reaction was quenched with 1 mL of $CHCl_3$ and the mixture centrifuged to remove the protein. The aqueous layer was adjusted to pH 9.0 with KOH and removed for ion-exchange chromatography. The NADD eluted in a large single peak with baseline separation from NAD-4d when eluted isocratically from an AG MP-1 column with 0.5 M NaCl in 100 mM KH_2PO_4 buffer (pH 10.0). The purified NADD was concentrated by rotary evaporation to a volume of 10 mL. The concentrated solution was then desalted via a Bio-Gel P-2 column. Fractions containing 0.6 mM NADD were subjected to ^{1}H NMR analysis. Analysis of the isotopic purity of NADD was carried out as described previously (*25*).

One dimensional ^{1}H NMR spectra were collected on a Varian VNMRS 500 MHz spectrometer operating at 499.88 MHz. Proton spectra were referenced to the residual water peak at 4.67 ppm. The spectra were collected using the PRESAT pulse sequence as provided by Varian, Inc., with a 90° pulse width; 128 and 17768 scans were used for NADH and NADD, respectively.

Data Processing. Data were analyzed using the appropriate rate equations and the Marquardt–Levenberg algorithm (*26*) supplied with EnzFitter from BIO-SOFT (Cambridge, U.K.)

and BASIC versions of the Fortran programs of Cleland (*27*). Data for saturation curves obtained with isocitrate as a substrate were fitted using eq 1, while data obtained with HIc and NAD as substrates were fitted using eq 2. Competitive inhibition patterns were fitted using eq 3, while data for *V* and *V*/*K* deuterium isotope effects were fitted using eq 4.

$$v = \frac{VA}{K_a + A} \quad (1)$$

$$v = \frac{VAB}{K_{ia}K_b + K_aB + K_bA + AB} \quad (2)$$

$$v = \frac{VA}{K_a\left(1 + \frac{I}{K_{is}}\right) + A} \quad (3)$$

$$v = \frac{VA}{K_a(1 + F_iE_{V/K}) + A(1 + F_iE_V)} \quad (4)$$

In eqs 1–4, v and V are initial and maximum velocities, respectively, A and B are substrate concentrations, I is the inhibitor concentration, K_a and K_b are Michaelis constants for substrates A and B, respectively, and K_{ia} is the dissociation constant for the EA complex. In eq 3, K_{is} represents the slope inhibition constant. In eq 4, F_i is the fraction of D_2O in the solvent or deuterium label in the substrate and $E_{V/K}$ and E_V are the isotope effects − 1 on *V*/*K* and *V*, respectively.

Data for pH−rate profiles or pK_i profiles with a limiting slope of 1 at low pH were fitted using eq 5, while data for pH−rate profiles with a limiting slope of −1 at high pH were fitted using eq 6. Data for pH−rate profiles that decreased with a limiting slope of 2 at low pH were fitted using eq 7, and data for pH−rate profiles that exhibit limiting slopes of 1 and −1 were fitted using eq 8. Data for pH−rate profiles with a slope of 1 at low pH and a partial change at high pH were fitted using eq 9.

$$\log y = \log\left[C/\left(1 + \frac{H}{K_1}\right)\right] \quad (5)$$

$$\log y = \log\left[C/\left(1 + \frac{K_2}{H}\right)\right] \quad (6)$$

$$\log y = \log\left[C/\left(1 + \frac{H}{K_1} + \frac{H^2}{K_1{}^2}\right)\right] \quad (7)$$

$$\log y = \log\left[C/\left(1 + \frac{H}{K_1} + \frac{K_2}{H}\right)\right] \quad (8)$$

$$\log y = \log\left\{\left[Y_L/\left(1 + \frac{H}{K_1}\right) + Y_H\left(\frac{K_2}{H}\right)\right]/\left(1 + \frac{K_2}{H}\right)\right\} \quad (9)$$

In eqs 5–9, y is the observed value of the parameter (V, V/K, or $1/K_i$) as a function of pH, C is the pH-independent value of y, H is the hydrogen ion concentration, K_1 and K_2 represent acid dissociation constants for enzyme or substrate functional groups important in a given protonation state for optimal binding and/or catalysis, Y_L is the pH-independent value of the partial change in the V/K_{NAD} pH−rate profile at low pH, and Y_H is the pH-independent value at high pH.

Table 1: Results of the HIc gCOSY Experiment

chemical shift	correlation
4.28 C(2)-H	2.86 C(3)-H
2.86 C(3)-H	1.90 C(4)-H, 1.80 C(4)-H
2.36 C(5)-H_2	1.90 C(4)-H, 1.80 C(4)-H
1.90 C(4)-H	2.86 C(3)-H, 2.36 C(5)-H_2, 1.80 C(4)-H
1.80 C(4)-H	2.86 C(3)-H, 2.36 C(5)-H_2, 1.90 C(4)-H

For the ^{13}C isotope effect studies, the data were fitted to eq 10:

$$(V/K) = \frac{\log(1 - f)}{\log[1 - f(R_f/R_0)]} \quad (10)$$

where f is the fraction of conversion of substrate to product, R_f is the isotope ratio of the CO_2 product at partial reaction, and R_0 is the isotope ratio determined from the total conversion experiments and represents the isotope ratio in the initial substrate.

Isotope ratios were given as $\delta^{13}C$ (eq 11, where R_{smp} and R_{std} are $^{13}C/^{12}C$ isotopic ratios for the sample and standard, respectively).

$$\delta^{13}C = (R_{smp}/R_{std} - 1) \times 10^3 \quad (11)$$

The standard for CO_2 was calibrated using Pee Dee Belemnite (*24*) with a $^{13}C/^{12}C$ ratio of 0.0112372.

RESULTS

Measurement of the Homoisocitrate pK_a by ^{1}H NMR. ^{1}H NMR spectra of HIc were obtained at pH 2.0 and 7.65 and referenced to HDO (4.68 ppm) (Figure 1A). Chemical shifts at pH 7.65 are as follows: δ 4.28 [d, 1H, C(2)-H], 2.86 [m, 1H, C(3)-H], 2.36 [m, 2H, C(5)-H_2], 1.82 [m, 2H, C(4)-H_2]. The ^{1}H NMR chemical shifts of HIc were assigned by gCOSY at pH 2.0 and 7.65. The correlations at pH 2.0 and 7.65 were identical, and those at pH 2.0 are listed in Table 1.

The chemical shifts of peaks corresponding to C(2)-H, C(3)-H, C(4)-H_2, and C(5)-H_2 changed significantly as the pH increased. The largest changes were seen for C(2)-H and C(3)-H, which shifted upfield by 0.50 and 0.60 ppm, respectively, as the pH was increased from 1.57 to 7.65. A plot of the chemical shift change of C(2)-H versus pH was used to estimate the pK_a values of HIc (Figure 1B). The pK_a values for the last two titratable groups of HIc are approximately 4.2 and 5.8, estimated by eye from Figure 1B as the pH that gives half the change in the two observable titration curves.

pH Dependence of Kinetic Parameters. The pH dependence of kinetic parameters reflects the optimum protonation state of enzyme and/or reactant functional groups required for enzyme conformation, binding, and/or catalysis. Initial velocity patterns were obtained as a function of pH by measuring the initial rate as a function of NAD concentration at different fixed levels of MgHIc or Ic (at a saturating level of Mg^{2+}). These patterns provide information about the kinetic mechanism as a function of pH. With HIc as a substrate, initial velocity patterns are consistent with the kinetic mechanism proposed previously (*2*), a steady-state random mechanism from pH 5.2 to 10.0. In addition, no change in kinetic mechanism was observed on the basis of the dead-end inhibition studies carried out at the extremes

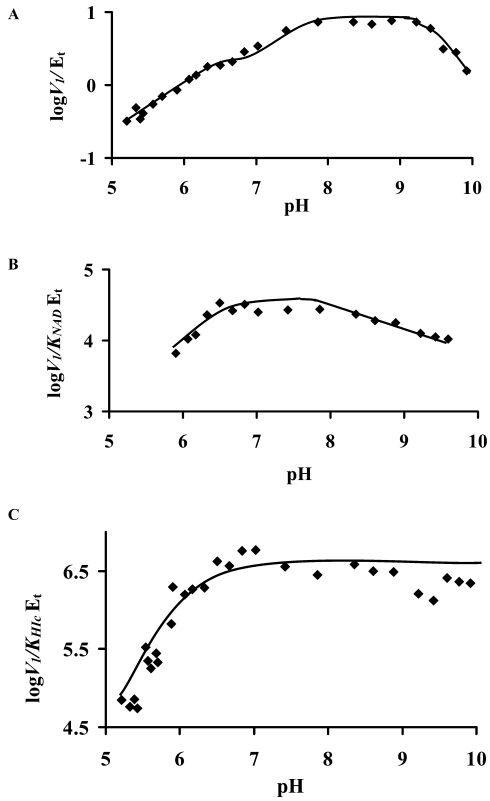

FIGURE 2: pH dependence of kinetic parameters for the HIcDH oxidative decarboxylation reaction of *S. cerevisiae* with HIc as the substrate determined at 25 °C for V_l/E_t (A), $V_l/K_{NAD}E_t$ (B), and $V_l/K_{MgHIc}E_t$ (C). The points shown are the experimentally determined values, while the curves are theoretical and based on fits of the data using eq 9 for $V_l/K_{NAD}E_t$ and eq 7 for $V_l/K_{MgHIc}E_t$. Data for V are discussed in the text.

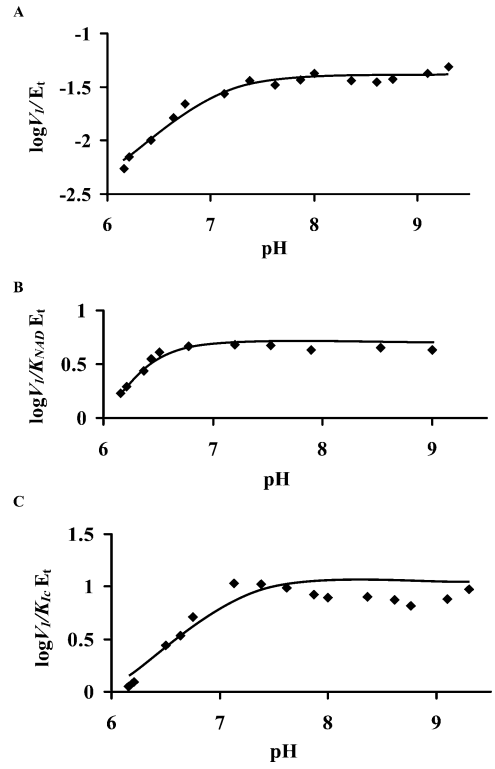

FIGURE 3: pH dependence of kinetic parameters for the HIcDH oxidative decarboxylation reaction of *S. cerevisiae* with isocitrate as the substrate determined at 25 °C for V_l/E_t (A), $V_l/K_{NAD}E_t$ (B), and $V_l/K_{Ic}E_t$ (C). The points shown are the experimentally determined values, while the curves are theoretical and based on fits of the data using eq 5.

of pH (5.2 and 10.0); this was also true with Ic as a substrate (rapid equilibrium random).

The pH dependencies of kinetic parameters for HIcDH with HIc and Ic as the substrates are shown in Figures 2 and 3, respectively. With HIc as a substrate, V_l/E_t decreases at low and high pH with limiting slopes of 1 and –1, respectively. Estimated pK_a values of 7.1 and 9.5 were obtained from a fit using eq 8. A hollow is observed in the curve as the pH decreases; i.e., the curve exhibits a plateau at pH 6.5, before it eventually decreases with a limiting slope of 1.[2] This aspect will be discussed further below. $V_l/K_{NAD}E_t$ decreases at low pH with a limiting slope of 1, giving a pK_a value of 6.4, while a partial change is observed at high pH giving a pK_a value of 8.3. $V_l/K_{MgHIc}E_t$ decreases at low pH with a limiting slope of 2, with an average pK_a value of 6.0. The pK_a values for the second and third ionizations of HIc are estimated to be 4.2 and 5.8, respectively, and thus, one of the groups observed in the $V_l/K_{MgHIc}E_t$ pH−rate profile likely reflects the substrate. All of the pK_a values are summarized in Table 2. Estimates of the pH-independent values of the kinetic parameters are as follows: $V_l/E_t = 9 \pm 0.1$ s^{-1}, $V_l/K_{NAD}E_t = (3.6 \pm 0.7) \times 10^4$ M^{-1} s^{-1}, and $V_l/K_{MgHIc}E_t = (3.9 \pm 0.3) \times 10^6$ M^{-1} s^{-1}. The pH-independent value of $V_l/K_{NAD}E_t$ at high pH is $(9.4 \pm 3.6) \times 10^3$ M^{-1} s^{-1}.

Table 2: pH Dependence of Kinetic Parameters for HIcDH from *S. cerevisiae*

		pK_a ± the standard error	
substrate	parameter	acid side	base side
isocitrate	V_l	6.9 ± 0.2	
	V_l/K_{NAD}	6.4 ± 0.3	
	V_l/K_{Ic}	7.1 ± 0.3	
HIc	V_l	7.1 ± 0.2	9.5 ± 0.2
	V_l/K_{NAD}	6.3 ± 0.5	8.3 ± 0.9
	V_l/K_{MgHIc}	6.0 ± 0.2[a]	
	pK_{iIc}	6.2 ± 0.1	
	pK_{iCPM}	6.5 ± 0.1	

[a] Average value.

With Ic as the substrate, the pH−rate profiles are simplified as a result of the equilibrium mechanism (*2*). V_l/E_t and $V_l/K_{Ic}E_t$ decrease at low pH, giving a limiting slope of 1 and a pK_a value of 6.9–7.1.[3] $V_l/K_{NAD}E_t$ also decreases at low pH but gives a pK_a of 6.4, 0.5 pH unit lower than that observed in the other two pH−rate profiles. pK_a values are summarized in Table 2. The pH-independent values of kinetic parameters are as follows: $V_l/E_t = 0.044 \pm 0.004$ s^{-1}, $V_l/K_{NAD}E_t = 5.9 \pm 0.8$ M^{-1} s^{-1}, and $V_l/K_{Ic}E_t = 14 \pm 2$ M^{-1} s^{-1}.

[2] Attempts to fit the data to eq 12 describing a hollow on the acid side of the pH−rate profile failed (*39*). A fit of eq 12 to the data is apparently not well conditioned. Apparent pK_a values were estimated from the crossover of the linear asymptotes with a slope of 1 (low pH) or –1 (high pH), with the asymptote of zero representing the pH-independent value of V/E_t.

[3] On the basis of isotope effect data, chemistry is rate-determining with isocitrate as the substrate. Although the $V/K_{Ic}E_t$ pH−rate profile appears to exhibit a "hump" at pH 7 (*40*), this is a result of error in the measurements at the high NAD concentrations used and the low activity of HIcDH with Ic (V/E_t is 200-fold lower and $V/K_{Ic}E_t$ 6000-fold lower than the corresponding values measured with Hic).

Scheme 2: Structure of the Inhibitor 3-Carboxypropylidenemalate (CPM)

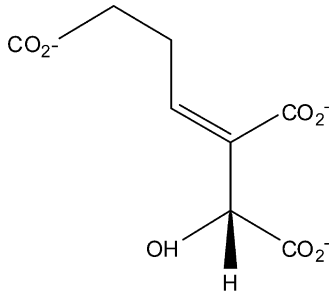

pH Dependence of the K_i for Ic. The pH dependence of the dissociation constant for competitive inhibitors versus HIc was determined to obtain an estimate of the true p*K* value(s) of group(s) required for optimum binding of reactants, and for comparison of apparent values seen for log V/K_{HIc} and log V/K_{Ic}. Ic (a slow substrate with 0.5% of the activity of HIc) or 3-carboxypropylidenemalate (CPM) (Scheme 2) was used as a dead-end inhibitor of HIc to measure pK_i profiles. Ic is competitive versus HIc over the pH range 5.26−9.22, and its pK_i profile is shown in Figure 4A. The K_i for Ic increases as the pH is decreased below 6.7, giving a pK_a of 6.2, estimated for the E−NAD complex, and the pH-independent value of K_{iIc} is 6.0 ± 0.1 mM. 3-Carboxypropylidenemalate is also a competitive inhibitor against HIc. Its pK_i profile is very similar to that of Ic; the pH-independent dissociation constant is 43 ± 7 μM, in agreement with that measured previously (*28*). The p*K* values are summarized in Table 2.

Primary Deuterium Kinetic Isotope Effects. With α-Ka and CO_2 as substrates, primary deuterium kinetic isotope effects [^{D}V and $^{D}(V/K_{CO_2})$] were measured by direct comparison of initial rates with A-side NADH(D) used as the labeled substrate. An isotope effect, within experimental error, equal to unity was measured for both of the kinetic parameters at pH 6.23, 7, 7.5, and 9.5.

With Ic as the substrate, primary deuterium kinetic isotope effects were measured by comparison of initial rates with *threo*-DL-isocitrate-2d as the labeled substrate at pH 8. Finite, and equal within error, isotope effects were observed; $^{D}V_1$ = 1.8 ± 0.2, and $^{D}(V_1/K_{Ic})$ = 1.7 ± 0.5.

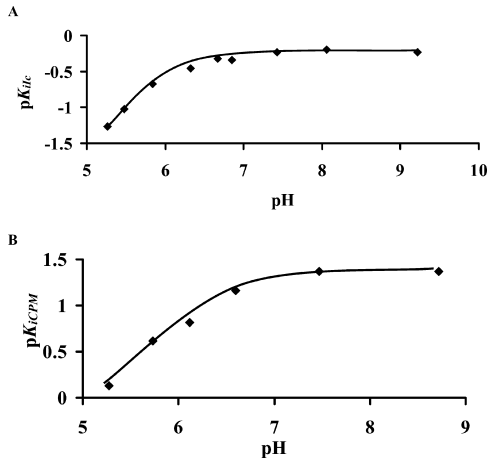

FIGURE 4: pH dependence of the reciprocal of the inhibition constant of isocitrate (A) and CMP (B). The points shown are the experimentally determined values, while the curves are theoretical and based on fits of the data using eq 5.

Effects of Solvent Deuterium and Viscosity. The pH(D) dependencies of kinetic parameters were measured at pH(D) values around 8 to determine whether a solvent isotope effect is observed using HIc or isocitrate as a substrate. Data are shown in Table 3. With HIc as the substrate, a normal solvent isotope effect is observed at pH 8, while the solvent effects are inverse using Ic as the substrate. Inverse isotope effects were also observed for the NAD-malic enzyme and were due to the effect of the increased viscosity of D_2O (η_{rel} = 1.24) (*29*).

Glycerol was used as a viscosogen for HIcDH. The effects of viscosity on kinetic parameters with glycerol as a viscosogen are given in Tables 3 and 4 and Figure 5. An increase in solvent viscosity generally results in an increase in *V* and *V*/*K* with Ic as the substrate (Table 3). The ratios of values of *V* and *V*/*K* determined in H_2O to the values determined in the presence of a viscosogen are, within error, equal to the corresponding solvent isotope effect. However, with HIc as the substrate, normal viscosity effects on *V* and V/K_{NAD} are observed, while an inverse viscosity effect was observed on V/K_{MgHIc}. Therefore, the values of observed solvent isotope effects, $^{D_2O}V_1$ and $^{D_2O}(V_1/K_{NAD})$, could result from a classical isotope effect and a normal viscosity effect, while the value of the observed isotope effect for V_1/K_{MgHIc} may be masked by an inverse viscosity effect. Correction of the Ic data for the viscosity effect gives a solvent isotope effect of 1 (Table 3). With HIc as the substrate, the viscosity dependence of kinetic constants is given in Table 4 and Figure 5. $^{\eta}V$ and $^{\eta}(V/K_{NAD})$ increased with an increase in solvent viscosity. However, viscosity has an only slight effect on V/K_{MgHIc}.

Multiple-Substrate Deuterium/^{13}C Kinetic Isotope Effects. The ^{13}C isotope effects on the oxidative decarboxylation of Ic or Ic-2d are as follows: $^{13}(V_1/K_{Ic})_H$ = 1.0311 ± 0.0002, and $^{13}(V_1/K_{Ic})_D$ = 1.0259 ± 0.0006, respectively, consistent with a stepwise oxidation decarboxylation.

Multiple-Solvent Deuterium/^{13}C Kinetic Isotope Effects. Multiple-isotope effects were used to define the interrelationship between the proton transfer and decarboxylation steps. The effect of the ^{13}C isotope on the oxidative decarboxylation of HIc in H_2O was 1.0057 ± 0.0003, while that measured in D_2O was 0.9972 ± 0.0004.

Determining the Stereospecificity of Hydride Transfer to NAD. To experimentally differentiate whether HIcDH is *pro-R* or *pro-S* specific for the transfer of hydride to NAD, the synthesized NAD-4d was used as the nucleotide for the reaction catalyzed by HIcDH with HIc as a substrate. If HIcDH is *pro-R* specific, [4*S*-^{2}H]NADH would be obtained. ^{1}H NMR was used to determine whether the NADD formed by HIcDH is [4*R*-^{2}H]- or [4*S*-^{2}H]NADH. The spectrum measured for the isolated NADD was compared to that of unlabeled NADH (*25*). In the ^{1}H NMR spectrum of unlabeled NADH, the two C4 protons of the dihydropyridine ring were clearly observed. The resonance centered at δ 2.47 (broad dd, *J* = 18.3, 1.5 Hz) is for the 4*S*-proton, and that centered at δ 2.60 (broad dt, *J* = 18.3, 2.5 Hz) is for the 4*R*-proton. The ^{1}H NMR spectrum of NADD generated from the HIcDH reaction indicates the presence of a broad doublet at δ 2.88 for the 4*R*-proton and loss of the signal at δ 2.73 for the 4*S*-proton, indicating the deuterium atom resides at the 4*S* position, indicative of 4*S*-NADD. The change in the chemical shift of NADD compared to that of NADH is likely a result

Table 3: Comparison of the Effects of Solvent and Viscosity on the Kinetic Parameters of HIcDH from *S. cerevisiae*

			H_2O/D_2O		H_2O/9% glycerol in H_2O	
fixed substrate	varied substrate	pH	$^{D_2O}V_1$	$^{D_2O}(V_1/K)$	V	V/K
MgHIc (80 μM)	NAD	8.0	2.6 ± 0.2	1.2 ± 0.2	1.5 ± 0.1	1.6 ± 0.2
NAD (8 mM)	MgHIc	8.0	2.5 ± 0.2	1.3 ± 0.2	1.5 ± 0.2	0.6 ± 0.1
Ic (50 mM)	NAD	8.0	0.82 ± 0.08 (1.2 ± 0.2)[a]	0.56 ± 0.09 (0.9 ± 0.2)[a]	0.7 ± 0.1	0.62 ± 0.07
NAD (30 mM)	Ic	8.0	0.94 ± 0.08 (1.4 ± 0.2)[a]	0.69 ± 0.08 (1.1 ± 0.2)[a]	0.66 ± 0.03	0.6 ± 0.1

[a] Values in parentheses are corrected for the viscosity effect with 9% glycerol.

Table 4: Viscosity Dependence of Kinetic Constants with HIc as the Substrate at pH 8.0

varied substrate	fixed substrate	n[a]	η_{rel}[b]	^nV[c]	$^n(V/K)$[c]
MgHIc	NAD (5 mM)	9%	1.24	1.39 ± 0.08	0.46 ± 0.08
		18%	1.7	2.4 ± 0.2	0.7 ± 0.2
		27%	2.15	3.8 ± 0.4	0.8 ± 0.4
NAD	MgHIc (80 μM)	9%	1.24	1.4 ± 0.1	1.88 ± 0.03
		18%	1.7	2.5 ± 0.2	2.9 ± 0.3
		27%	2.15	4.4 ± 0.5	5 ± 1

[a] Fraction of glycerol in H_2O. [b] The relative viscosity of glycerol, which is the ratio of the absolute viscosity of a solution containing the viscosogen to the absolute viscosity of water at 25 °C. [c] The ratio of V and V/K at 100% H_2O to that at n fraction of glycerol.

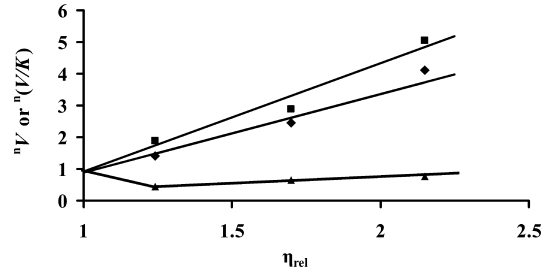

FIGURE 5: Effect of viscosity on kinetic parameters with glycerol as the viscosogen. Ratios of V and V/K at 100% H_2O to that at n fraction of glycerol vs the relative viscosity of glycerol [^nV (◆), $^n(V/K_{MgHIc})$ (▲), and $^n(V/K_{NAD})$ (■)]. The points are experimental, while the lines are based on linear fits of the data.

of the high concentration of metal ions in the NADD solution. Therefore, HIcDH is *pro-R* specific for hydride transfer, identical to the stereospecificity of IcDH (*30*).

DISCUSSION

Multiple-Substrate Deuterium/^{13}C Kinetic Isotope Effects. Multiple-isotope effects allow one to distinguish between a concerted and stepwise mechanism and provide estimates of the intrinsic isotope effects on the bond-breaking steps (*23*). Three isotope effects were measured with Ic as the substrate, $^D(V/K_{Ic})$, $^{13}(V_1/K_{Ic})_H$, a ^{13}C isotope effect using Ic-2h, and $^{13}(V_1/K_{Ic})_D$, a ^{13}C isotope effect with Ic-2d. If $^{13}(V_1/K)_D$ is equal to or greater than $^{13}(V_1/K)_H$, the deuterium and ^{13}C isotope effects are in the same step, which indicates the reaction is concerted. If the step is completely rate-limiting, the ^{13}C isotope effect measured with Ic-2d will not change in the presence of the second isotope, while if the chemical step is not completely rate-limiting with the protium-labeled reactant, the isotope effect will increase. A decrease in $^{13}(V_1/K)_D$ compared to $^{13}(V_1/K)_H$ demonstrates a stepwise mechanism (*23*). Deuteration of the substrate decreases the observed isotope effect by increasing the rate limitation of the hydride transfer step.

Ic is a slow substrate for the reaction catalyzed by HIcDH; that is, the rates of chemical steps with this substrate are much slower than that with HIc as the substrate ($V/K_{MgHIc}E_t$ is 3×10^5-fold greater than $V/K_{Ic}E_t$). The kinetic mechanism is equilibrium random compared to the steady-state random mechanism observed with HIc (*2*). With Ic as the substrate, the oxidative decarboxylation reaction catalyzed by HIcDH is stepwise with oxidation preceding decarboxylation. Both hydride transfer and decarboxylation steps contribute significantly to the rate limitation of the reaction, given values of 1.7–1.8 for ^DV and $^D(V/K)$ and 1.031 for $^{13}(V/K)$. A value of 1.05 (^{13}k) has been measured for the metal-catalyzed decarboxylation of oxaloacetate, and thus, 1.03 is a large ^{13}C isotope effect suggesting decarboxylation contributes more {~60%; $[^{13}(V/K) - 1]/(^{13}k - 1) \times 100$} to overall rate limitation at a limiting level of Ic.

With HIc as the substrate, a primary deuterium isotope effect of 1 was observed with A-side NADD over the pH range of 6.2−9.5. It was thought that the isotope effect might be increased at low pH because catalysis would be slowed and the commitment to catalysis would be weakened. However, the related IcDH reaction exhibits very small deuterium and ^{13}C isotope effects (*31*). In addition, the V/K_{Ic} decreases at low pH with a limiting slope of 2 (*32*), with the first pK reflecting a substrate carboxylate, which must be ionized for optimum binding, and the lowest pK_a reflecting a catalytic group. The ^{13}C effect does not increase until the pH decreases below the pK_a for the catalytic group (*31*). In the V/K_{HIc} pH−rate profile, there are two groups on the acid side with an average pK value of 6.0. The phenomenon is likely the same as that for IcDH. On the basis of these studies, it can be stated that the oxidative decarboxylation portion of the reaction provides only a minor contribution to the rate limitation of the overall reaction with the natural substrate.

Solvent Deuterium Kinetic Isotope Effects. With HIc as a substrate for the oxidative decarboxylation reaction catalyzed by HIcDH, the observed values of the solvent deuterium kinetic isotope effects (SKIEs), $^{D_2O}V_1$ and $^{D_2O}(V_1/K)$, were normal, although $^{D_2O}(V_1/K)$ values were near unity (Table 3). However, with Ic as the substrate, inverse solvent isotope effects were observed. Ic is a slow substrate, as discussed above, and one would predict equal and normal isotope effects on V and V/K in a rapid equilibrium random mechanism if proton transfer occurs in the rate-limiting transition state(s). Although equal, inverse SKIEs were obtained on V and V/K_{Ic}, which might be attributed to one of several possibilities: (A) ionization of a thiol, (B) a medium effect, (C) hydrolysis of a metal-chelated water, or (D) a change in solvent viscosity resulting from substitution of D_2O for H_2O ($\eta_{rel} = 1.24$) (*29*). Cysteine is the only amino acid with a side chain that has an exchangeable hydrogen with a fractionation factor of <1 (~0.5) (*20*). A comparison of the protein sequences of HIcDH from *S. cerevisiae* and

Thermus thermophilus and on the basis of the crystal structure of the HIcDH from *T. thermophilus*, no cysteine is located in the active site.[4] Hydrolysis of metal-bound water is unlikely, while the presence of a medium effect is possible.

The change in solvent viscosity that results from substitution of D_2O for H_2O can account for the inverse solvent isotope effect. The solvent isotope effects are listed in Table 3 and are compared to the effects caused by the presence of glycerol as a viscosogen at a relative viscosity identical to that of D_2O. The changes in the kinetic parameters at increased viscosity are identical, within error, to the changes observed in D_2O, strongly suggesting the inverse isotope effects are a consequence of the change in solvent viscosity. Eliminating the viscosity effects from the observed solvent isotope effects gives the corrected data shown in Table 3. Effects near unity suggest proton transfer steps do not contribute or contribute to a very small extent to the rate limitation in the reaction with Ic as the substrate. The reason for the increased rate in the presence of a viscosogen is not known at this point but may result from stabilization of an enzyme conformation along the reaction pathway of HIcDH.

The increase in the solvent viscosity in D_2O affects the reaction with HIc as a substrate differently, giving a decrease in V and V/K_{NAD} that is proportional to increased solvent viscosity, that is, a normal viscosity effect. However, the viscosity effect on V/K_{MgHIc} is inverse. HIcDH has a steady-state random kinetic mechanism with a preferred binding of MgHIc before NAD (*2*). Data suggest MgHIc binding generates the active conformation, a slow step along the reaction pathway. The inverse viscosity effect may thus be due to stabilization of the enzyme conformation that exists when MgHIc binds to the E or E−NAD complex. Thus, V and V/K_{NAD} do not exhibit the inverse solvent isotope effect, but V/K_{MgHIc} does. The normal viscosity effect observed on V/K_{NAD} is likely indicative of a diffusion-limiting step in V/K, likely NAD binding consistent with the linear dependence of the rate constant on η_{rel} (Figure 5). The normal viscosity effect on V likely results from a contribution of product release to rate limitation. Viscosity has an only slight, if any, effect on V/K_{MgHIc} which remains inverse at all glycerol concentrations.

The effects of solvent deuterium observed in these studies indicate that the observed SKIE is likely a mixture of a normal SKIE and solvent viscosity effects. In the malic enzyme reaction, D_2O also functioned as a viscosogen (*29*). On the basis of the studies of the effects of solvent deuterium and viscosity, and the similar effects observed in other systems, it is apparent that viscosity effects should be checked routinely as one measures solvent deuterium kinetic isotope effects.

Multiple-Solvent Deuterium/^{13}C Kinetic Isotope Effects. The primary ^{13}C isotope effect measured with HIc as the substrate is 0.5% in H_2O. The small value indicates, as stated above, that decarboxylation contributes only slightly to rate limitation $\{[^{13}(V/K) - 1]/(^{13}k - 1) \times 100 = 11\%\}$.

In D_2O, however, an inverse value of $^{13}(V/K)$ is observed. With HIc as the substrate, the slow step under V/K conditions is almost certainly a conformational change induced by HIc prior to catalysis as suggested above. As a result, in D_2O the binding of HIc will likely come to equilibrium, and the inverse ^{13}C isotope effect likely suggests a binding isotope effect. A similar effect has been observed for 6-PGDH in the presence of 3-acetylpyridine adenine dinucleotide 2′-phosphate (APADP) with 6-phosphogluconate deuterated at C3 (6PG-3d) (*33*). In this case, the effect was ascribed to a change in torsional modes, such as rotation of the β-carboxylate and/or the C2−C3 bond of HIc. At any rate, there must be an increase in the fractionation factor of the carboxylate carbon upon binding of HIc.

Conclusions about Isotope Effects. Isotope effect data with Ic as the substrate suggest the chemical steps are rate-limiting in the reaction. The multiple-substrate deuterium/^{13}C isotope effects indicate a stepwise mechanism. Proton transfer steps do not contribute to the rate limitation or are compensated by the inverse viscosity effect, and no SKIE is observed. Proton transfer does occur in both hydride transfer and decarboxylation steps; therefore, either the proton has already been transferred in the transition state, or a normal SKIE is offset by the viscosity effect. Data obtained are very similar to those of the malic enzyme, where both hydride transfer and decarboxylation steps contribute to the rate limitation, and the decarboxylation step is the more rate-limiting of the two (*34, 35*). With HIc as the substrate, isotope effect data suggest the chemical step contributes only slightly to rate limitation. On the basis of data from solvent isotope effects, viscosity effects, and multiple-solvent/^{13}C isotope effects, the proton transfer step(s) is slow but likely reflects an enzyme conformational change.

Enzymes that catalyze β-hydroxy acid oxidative decarboxylation that have been studied include NAD(P)-malic enzyme (*31, 35*), NADP-dependent IcDH (*31*), 6-PGDH (*36, 37*), and TDH (*38*). These enzymes have the same general acid–base mechanism (Scheme 1). With Ic as the substrate, the oxidative decarboxylation reaction catalyzed by HIcDH is stepwise with hydride transfer preceding decarboxylation which is the same as that of the proteins mentioned above with NAD(P) as the dinucleotide substrate (*23, 31, 35–39*). Both steps contribute to the rate limitation of the reaction. However, the situation is different with HIc as the substrate, with a conformational change prior to the chemical steps being rate-limiting overall.

Interpretation of the pK_i Profile. The apparent pK is displaced from its true value in the V/K profile of a sticky substrate. The true value can be estimated from the pK_i profile of a competitive inhibitor, or the V/K profile of a nonsticky substrate. The pK_i profile for isocitrate and CPM, competitive inhibitors of HIc, gave pK_a values of 6.2–6.5. This is, within error, identical to the pK_a observed in the V/K_{NAD} pH−rate profile. However, it is apparently 0.5 pH units lower than that observed in the V and V/K_{Ic} pH−rate profiles.

Interpretation of the pH Dependence of Kinetic Parameters with Ic as the Substrate. Isocitrate is a slow nonsticky substrate, with a catalytic rate decreased 200-fold (V/E_t) compared to that of HIc (*2*). A rapid equilibrium random kinetic mechanism is observed with Ic (*2*), and the interconversion of the central complexes is likely rate-limiting. The pK_a of 6.9–7.1 observed in V_1/E_t and $V_1/K_{Ic}E_t$ profiles is likely that of a general base that accepts a proton from Ic as it is oxidized. Given the equilibrium random nature of

[4] Sequence alignment indicates the *S. cerevisiae* and *T. thermophilus* HIcDHs are 44.5% identical and all of the active site residues are conserved (*41*).

Scheme 3: Mechanism for HIcDH that Allows for Binding of the Substrate to E and EH

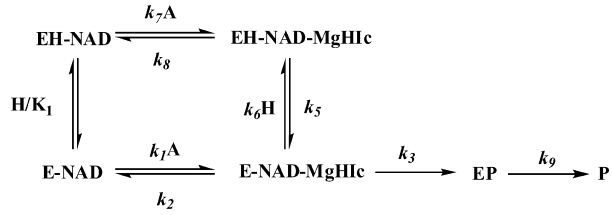

the mechanism, the group with a pK_a of 6.4 in $V_l/K_{NAD}E_t$ reflects the same group observed in V_l/E_t and $V_l/K_{Ic}E_t$ profiles; the error in these measurements is greater than those with HIc. The pK_a value observed in the $V_l/K_{Ic}E_t$ profile represents the enzyme group in the E−Mg−NAD complex, while that observed in the $V_l/K_{NAD}E_t$ profile represents the same group in the E−Mg−Ic complex. Thus, a pK_a of 6.5 (pK_i profile) to 7 (V_l/E_t and $V_l/K_{Ic}E_t$ profiles) is estimated for the general base that accepts a proton from the β-hydroxy acid of either Ic or HIc in the hydride transfer step.

Interpretation of the pH Dependence of Kinetic Parameters with HIc as the Substrate. With HIc as the substrate, because of its stickiness, the shapes of the pH−rate profiles are more complex. A hollow is observed on the acid side of the V pH−rate profile, giving a pK_a of 7 estimated by fitting to eq 8, which assumes no hollow in the profile. A hollow occurs when the substrate and proton are sticky in the ternary E−NAD−MgHIc complex (*10*), or from a combination of effects of a partial change resulting from a change in the rate-limiting step and protonation of the general base. Given the steady-state random nature of the mechanism, it is likely that substrate and proton stickiness generates the hollow in this case. Equation 12 is applicable for the case in which both the substrate and the proton in EAH are sticky (Scheme 3). If pK_2 is less than 7.3, eq 13 can apply for analysis of the hollow (*40*).

$$v/E_t = \{[k_3k_9/(k_3 + k_9)](1 + H/K_\alpha)\}/\{1 + (k_3k_5k_8 + k_5k_8k_9 + k_3k_8k_9 + k_2k_8k_9 + k_2k_5k_9)(H/K_2) + k_5k_8k_9(H/K_2)^2/[k_2(k_5 + k_8)(k_3 + k_9)]\} \quad (12)$$

$$\text{app p}K = \text{p}K_2 - \log\left(\frac{1 + \frac{k_3}{k_9}}{1 + \frac{k_3}{k_2 + k_6}}\right) \quad (13)$$

In this case, K_α in eq 12 is $(k_2/k_8)(1 + k_8/k_5)K_2$, the app p$K$ in eq 13 is the crossover point of the limiting asymptotes (slope of 1 and slope of 0) in Figure 2A, and pK_2 is the acid dissociation constant for the EH−NAD−MgHIc complex, the intrinsic pK_a, which is 7 from the V profile with Ic as the substrate. A viscosity effect is observed on V with HIc as the substrate, suggesting the reaction must be at least partially limited by product release; i.e., $k_3 > k_9$ in Scheme 3. In addition, the substrate and proton must be sticky to generate a hollow, and $k_3 > k_2 + k_6$. Equation 13 then reduces to app pK = pK_2 − log[$(k_2 + k_6)/k_9$]. The app pK is 7 and is approximately equal to the intrinsic pK_a, giving k_9 approximately equal to $k_2 + k_6$. Thus, the rate of the product release step is equal to or greater than the rate of dissociation of the substrate from or protonation of the E−NAD−MgHIc complex (Scheme 3).

The group with a pK_a on the base side was observed only in the V pH−rate profile for HIc. No change in kinetic mechanism was observed for HIcDH over the entire pH range that was studied. Product release is known to contribute to rate limitation at neutral pH, and the large SKIE observed on V may result from a pH dependence of the product release step or tautomerization of the enol to the ketone product. The most likely of the two is the latter, and the pK_a of 9.5 would reflect the general acid that protonates the enol.

The $V_l/K_{NAD}E_t$ pH−rate profile exhibits a group with a pK_a of 6.4 at low pH, similar to that observed in the $V_l/K_{NAD}E_t$ profile with Ic as the substrate. This group, in the E−MgHIc complex, likely reflects the general base, as it does in the V_l/E_t, $V_l/K_{NAD}E_t$, and $V_l/K_{Ic}E_t$ profiles obtained with Ic as the substrate. Thus, NAD is likely not very sticky in the E−NAD−MgHIc complex, while MgHIc is, consistent with the slow conformational change elicited by substrate binding (see the isotope effects described above).[5] A partial change in the second-order rate constant is observed at high pH, giving a pK_a of 8.3 and an approximately 4-fold decrease in rate. The reason for the partial change is not known at this point but may result from a decrease in the affinity of NAD upon deprotonation of an enzyme group with a pK_a of 8.3 or a pH-dependent conformational change. The reason will have to await further study.

The V_l/K_{HIc} pH−rate profile shows two groups on the acid side with an average pK_a of 6.0. One group is likely the third pK_a of HIc on the basis of the measured pK_a of 5.8 for HIc. The substrate carboxylate pK_a was not observed in the V_l/K_{Ic} pH−rate profile because Ic is a poor substrate and the pK_a was outside the range of our measurements. The second group is likely the general base. The pK_a of 6 is 1 pH unit lower than that observed in the V_l/K_{Ic} pH−rate profile. Since the latter is almost certainly an intrinsic pK_a, the stickiness factor for MgHIc can be determined from the following expression (*40*).

$$\text{app p}K_a = \text{p}K_a - \log(1 + S_r) \quad (14)$$

where S_r is the stickiness factor. S_r is thus 9; that is, the net rate constant for catalysis is 9 times greater than the net off rate for dissociation of MgHIc from the E−NAD−MgHIc complex.

Proposed Chemical Mechanism. The pH−rate profiles and isotope effect experiments discussed above are consistent with the chemical mechanism shown in Scheme 1. Two groups act as acid–base catalysts in the reaction on the basis of the pH−rate profiles. A group with a pK_a of 6.5–7 serves as a general base catalyst in the reaction. This residue likely accepts a proton as the β-hydroxy acid is oxidizd to the β-keto acid. The group participates in all three steps to shuttle the proton between the C2 hydroxyl and itself. The second group, acting as a general acid with a pK_a of 9.5, likely catalyzes the tautomerization step by donating a proton to the enol to give the final product. However, this group is observed only in the V profile with HIc as the substrate, and

[5] The forward commitment factor includes an internal term reflecting the ratio of the rate constant for the chemical step to that of the reverse conformational change and an external term reflecting substrate stickiness. Thus, even in a case where the substrate is not sticky, a large internal commitment factor will result in a primary isotope effect of 1. In the case presented here, the primary isotope effect is pH-independent and equal to 1.

not in the profiles with Ic as the substrate. The general acid catalyzes the tautomerization step with both substrates but is not observed with Ic because the oxidative decarboxylation portion of the reaction limits overall.

A multiple-sequence alignment of HIcDH from *S. cerevisiae* and *T. thermophilus*, IcDH from *Escherichia coli*, and IPMDH from *Thiobacillus ferrooxidans* has been carried out. Lys and Tyr are conserved in the active sites of all of the enzymes and may serve as the catalytic groups. The Tyr residue, Y140 in IPMDH and Y160 in IcDH, extends its side chain toward the substrate in position to act as a base in the oxidation step or an acid after decarboxylation (*41*). In the HIcDH from *T. thermophilus*, kinetic analysis of the Y125A mutant enzyme gave a decrease of 8-fold in k_{cat}, but K_m for Ic increased slightly. Data suggested that Y125 was also involved in the catalytic process (*42*). In addition, Y139 (a Y125 homologue) in *T. thermophilus* IPMDH was proposed to be a catalytic residue (*43*). This Tyr could thus be the general acid with a pK_a of 9.5 observed in the *V* pH−rate profile. Lysine 212 is required for the catalytic activity of porcine NADP-dependent IcDH (*41*). At pH 7.4, the specific activity is decreased in the K212Q, K212Y, and K212R mutants by comparison with that of the wild type to 0.01–9%. In agreement, site-directed mutagenesis indicated K230 was a catalytic residue in the IcDH from *E. coli* (*44*). Thus, Lys may be the general base with a pK_a of 6.4 in HIcDH. Further studies with HIcDH, including site-directed mutagenesis, are now in progress.

REFERENCES

1. Strassman, M., and Ceci, L. N. (1965) Enzymatic formation of α-ketoadipate acid from homoisocitric acid. *J. Biol. Chem. 240*, 4357–4361.
2. Lin, Y., Alguindigue, S. S., Volkman, J., Nicholas, K. M., West, A. H., and Cook, P. F. (2007) The complete kinetic mechanism of homoisocitrate dehydrogenase from *Saccharomyces cerevisiae*. *Biochemistry 46*, 890–898.
3. Chen, R., and Yang, H. (2000) A highly specific monomeric isocitrate dehydrogenase from *Corynebacterium glutamicum*. *Arch. Biochem. Biophys. 383*, 238–245.
4. Grodsky, N. B., Soundar, S., and Colman, R. F. (2000) Evaluation by site-directed mutagenesis of aspartic acid residues in the metal site of pig heart NADP-dependent isocitrate dehydrogenase. *Biochemistry 39*, 2193–2200.
5. Rabin, R., Salamon, I. I., Bleiweis, A. S., Carlin, J., and Ajl, S. J. (1968) Metabolism of ethylmalic acids by *Pseudomonas aeruginosa*. *Biochemistry 7*, 377–388.
6. Pirrung, M. C., Han, H., and Nunn, D. S. (1994) Kinetic mechanism and reaction pathway of *Thermus thermophilus* isopropylmalate dehydrogenase. *J. Org. Chem. 59*, 2423–2429.
7. Veiga Salles, J. B., and Ochoa, S. (1950) Biosynthesis of dicarboxylic acids by carbon dioxide fixation. II. Further study of the properties of the "malic" enzyme of pigeon liver. *J. Biol. Chem. 187*, 849–861.
8. Hsu, R. Y., and Lardy, H. A. (1967) Pigeon liver malic enzyme. II. Isolation, crystallization, and some properties. *J. Biol. Chem. 242*, 520–526.
9. Tipton, P. A., and Peisach, J. (1990) Characterization of the multiple catalytic activities of tartrate dehydrogenase. *Biochemistry 29*, 1749–1756.
10. Price, N. E., and Cook, P. F. (1996) Kinetic and chemical mechanisms of the sheep liver 6-phosphogluconate dehydrogenase. *Arch. Biochem. Biophys. 336*, 215–223.
11. Silverberg, M., and Dalziel, K. E. (1973) Crystalline 6-phosphogluconate dehydrogenase from sheep liver. *Eur. J. Biochem. 38*, 229–238.
12. Karsten, W. E., Liu, D., Rao, G. S., Harris, B. G., and Cook, P. F. (2005) A catalytic triad is responsible for acid-base chemistry in the *Ascaris suum* NAD-malic enzyme. *Biochemistry 44*, 3626–3635.
13. Karsten, W. E., Chooback, L., and Cook, P. F. (1998) Glutamate 190 is a general acid catalyst in the 6-phosphogluconate-dehydrogenase-catalyzed reaction. *Biochemistry 37*, 15691–15697.
14. Zhang, L., Chooback, L., and Cook, P. F. (1999) Lysine 183 is the general base in the 6-phosphogluconate dehydrogenase-catalyzed reaction. *Biochemistry 38*, 11231–11238.
15. Viola, R. E., Cook, P. F., and Cleland, W. W. (1979) Stereoselective preparation of deuterated reduced nicotinamide adenine nucleotides and substrates by enzymatic synthesis. *Anal. Biochem. 96*, 334–340.
16. Ma, G., and Palmer, D. R. J. (2000) Improved asymmetric syntheses of (*R*)-(−)-homocitrate and (2*R*,3S)-(−)-homoisocitrate, intermediates in the α-aminoadipate pathway of fungi. *Tetrahedron Lett. 41*, 9209–9212.
17. O'Leary, M. H., and Limburg, J. A. (1977) Isotope effect studies of the role of metal ions in isocitrate dehydrogenase. *Biochemistry 16*, 1129–1135.
18. Friedman, L., and Kosower, E. (1955) *Organic Syntheses*, Collect. Vol. III, p 510, Wiley, New York.
19. Schowen, K. B., and Schowen, R. L. (1982) Solvent isotope effects on enzyme systems. *Methods Enzymol. 87*, 551–606.
20. Quinn, D. M., and Sutton, L. D. (1991) in *Enzyme Mechanism from Isotope Effects* (Cook, P. F., Ed.) pp 73–126, CRC Press, Boca Raton, FL.
21. Bazelyansky, M., Robey, E., and Kirsch, J. F. (1986) Fractional diffusion-limited component of reactions catalyzed by acetylcholinesterase. *Biochemistry 25*, 125–130.
22. O'Leary, M. H. (1980) Determination of heavy-atom isotope effects on enzyme-catalyzed reactions. *Methods Enzymol. 64*, 83–104.
23. Hermes, J. D., Roeske, C. A., O'Leary, M. H., and Cleland, W. W. (1982) Use of multiple isotope effects to determine enzyme mechanisms and intrinsic isotope effects. Malic enzyme and glucose-6-phosphate dehydrogenase. *Biochemistry 21*, 5106–5114.
24. Craig, N. (1957) Isotopic standard for carbon and oxygen and correction factors for mass-spectrometric analysis of carbon dioxide. *Geochim. Cosmochim. Acta 12*, 133–149.
25. Moinuddin, S. G. A., Youn, B., Bedgar, D. L., Costa, M. A., Helms, G. L., Kang, C., Davin, L. B., and Lewis, N. G. (2006) Secoisolariciresinol dehydrogenase: Mode of catalysis and stereospecificity of hydride transfer in *Podophyllum peltatum*. *Org. Biomol. Chem. 4*, 808–816.
26. Marquardt, D. W. (1983) An algorithm for least square estimation of nonlinear parameters. *J. Soc. Ind. Appl. Math. 11*, 431–441.
27. Cleland, W. W. (1979) Statistical analysis of enzyme kinetic data. *Methods Enzymol. 63*, 103–108.
28. Yamamoto, T., Miyazaki, K., and Eguchi, T. (2007) Substrate specificity analysis and inhibitor design of homoisocitrate dehydrogenase. *Bioorg. Med. Chem. 15*, 1346–1355.
29. Karsten, W. E., Lai, C., and Cook, P. F. (1995) Inverse solvent isotope effects in the NAD-malic enzyme reaction are the result of the viscosity difference between D_2O and H_2O: Implications for solvent isotope effect studies. *J. Am. Chem. Soc. 117*, 5914–5918.
30. Nakamoto, T., and Vennesland, B. (1960) The enzymatic transfer of hydrogen. VIII. The reactions catalyzed by glutamic and isocitric dehydrogenases. *J. Biol. Chem. 235*, 202–204.
31. Grissom, C. E., and Cleland, W. W. (1988) Isotope effect studies of chemical mechanism of pig-heart NADP isocitrate dehydrogenase. *Biochemistry 27*, 2934–2943.
32. Cook, P. F., and Cleland, W. W. (1981) pH variation of isotope effects in enzyme-catalyzed reactions. 1. Isotope- and pH-dependent steps the same. *Biochemistry 20*, 1797–1805.
33. Hwang, C., Berdis, A. J., Karsten, W. E., Cleland, W. W., and Cook, P. F. (1998) Oxidatice decarboxylation of 6-phosphogluconate dehydrogenase proceeds by a stepwise mechanism with NADP and ADADP as oxidants. *Biochemistry 37*, 12596–12602.
34. Kiick, D. M., Harris, B. G., and Cook, P. F. (1986) Protonation mechanism and location of rate-determining steps for the *Ascaris suum* nicotinamide adenine dinucleotide-malic enzyme reaction from isotope effects and pH studies. *Biochemistry 25*, 227–236.
35. Weiss, P. M., Gavva, S. R., Harris, B. G., Urbauer, J. C., Cleland, W. W., and Cook, P. F. (1991) Multiple isotope effects with alternative dinucleotide substrates as a probe of the malic enzyme reaction. *Biochemistry 30*, 5755–5763.
36. Rendina, A. R., Hermes, J. D., and Cleland, W. W. (1984) Use of multiple isotope effects to study the mechanism of 6-phosphogluconate dehydrogenase. *Biochemistry 23*, 6257–6262.

37. Berdis, A. J., and Cook, P. F. (1993) Chemical mechanism of 6-phosphogluconate dehydrogenase from *Candida utilis* from pH studies. *Biochemistry 32*, 2041–2046.
38. Tipton, P. A. (1996) Transient-state kinetic analysis of the oxidative decarboxylation of D-malate catalyzed by tartrate dehydrogenase. *Biochemistry 35*, 3108–3114.
39. Grissom, C. E., and Cleland, W. W. (1988) Isotope effect studies of chicken liver NADP malic enzyme: Role of the metal ion and viscosity dependence. *Biochemistry 27*, 2927–2934.
40. Cook, P. F., and Cleland, W. W. (2007) *Enzyme kinetics and mechanism*, pp 354–357, Taylor & Francis Group, LLC, London.
41. Kim, T. K., Lee, P., and Colman, R. F. (2003) Critical role of Lys212 and Tyr140 in porcine NADP-dependent isocitrate dehydrogenase. *J. Biol. Chem. 278*, 49323–49331.
42. Miyazaki, J., Asada, K., Fushinobu, S., Kuzuyama, T., and Nishiyama, M. (2005) Crystal structure of tetrameric homoisocitrate dehydrogenase from an extreme thermophile, *Thermus thermophilus*: Involvement of hydrophobic dimer-dimer interaction in extremely high thermotolerance. *J. Bacteriol. 187*, 6779–6788.
43. Miyazaki, K., and Oshima, T. (1993) Tyr-139 in *Thermus thermophilus* 3-isopropylmalate dehydrogenase is involved in catalytic function. *FEBS Lett. 332*, 37–38.
44. Lee, M. E., Dyer, D. H., Klein, O. D., Bolduc, J. M., Stoddard, B. L., and Koshland, D. E., Jr. (1995) Mutational analysis of the catalytic residues lysine 230 and tyrosine 160 in the $NADP^+$-dependent isocitrate dehydrogenase from *Escherichia coli*. *Biochemistry 34*, 378–384.

BI702361J